ORIGINAL RESEARCH COMMUNICATION

Crucial role of Flvcr1a in the maintenance of intestinal heme homeostasis

SHORT TITLE: Role of Flvcr1a in mouse intestine

Veronica Fiorito[1,2], Marco Forni[3], Lorenzo Silengo[1,2], Fiorella Altruda[1,2] and Emanuela Tolosano[1,2]

[1]Molecular Biotechnology Center, University of Torino, 10126, Torino, Italy

[2]Department of Molecular Biotechnology and Health Sciences, University of Torino, 10126, Torino, Italy

[3] EuroClone S.p.A Research Laboratory, Molecular Biotechnology Centre (MBC), University of Torino, 10126, Torino, Italy

CORRESPONDENCE:

Emanuela Tolosano, PhD

Molecular Biotechnology Center

Dept. Molecular Biotechnology and Health Sciences

Via Nizza 52

10126 Torino, Italy

Phone: +39-011-6706423

Fax: +39-011-6706432

email: emanuela.tolosano@unito.it

WORD COUNT: 5976

REFERENCE NUMBER: 35

GREYSCALE ILLUSTRATIONS: 4

COLOR ILLUSTRATIONS: 3 (hardcopy)

ABSTRACT

Aims. The maintenance of heme homeostasis, mucosa cell renewal and redox environment in the intestine is essential to permit digestion, absorption, cell proliferation, cell apoptosis, and immune response and to avoid the development of gut disorders.

The Feline Leukemia Virus, subgroup C, Receptor 1a (FLVCR1a) is a heme exporter expressed in almost all cell types including intestinal cells.

This work investigates the role of FLVCR1a in the intestine taking advantage of an intestine specific conditional Flvcr1a-knockout mouse and of Flvcr1a-depleted Caco2 cells.

Results. The data show that FLVCR1a does not participate in the absorption of dietary heme, whereas it is involved in the export of *de novo* synthesized heme from intestinal cells. The loss of Flvcr1a is associated to a decrease of intestinal cell proliferation and to alterations in the peculiar homeostasis of proliferating cells, including the maintenance of their redox status. The involvement of Flvcr1a in these processes renders this exporter crucial for the survival of mice in a model of ulcerative colitis.

Innovation. These findings shed light on the role of heme export in the dietary heme absorption process and unravel a new role for heme export in the control of mucosal renewal and in proliferating cell redox status and metabolic activity, demonstrating a crucial role for FLVCR1a in maintaining intestinal homeostasis in both physiologic and pathologic situations.

Conclusion. By exporting the excess of *de novo* synthesized heme from intestinal cells, FLVCR1a participates in the control of intestinal mucosa homeostasis.

INTRODUCTION

Heme, a complex of iron with protoporphyrin IX, is ubiquitous in aerobic cells and it plays pivotal roles in many cellular processes. First, heme acts as an important cofactor in oxygen transport and storage, being a constitutive element of hemoglobin and myoglobin. Moreover, mitochondrial electron transport depends on heme-containing protein complexes(3). Furthermore, heme availability is crucial for the activity of cytochromes, important for drug and steroid metabolism, as well as for that of enzymes involved in signal transduction, like nitric oxide synthases or soluble guanylate cyclases. Heme can also regulate the transcription of many target genes, including antioxidant-defence enzymes. Finally, heme intracellular localization (cytosolic vs. nuclear) and concentration affects gene transcription and translation(4,16). Besides these beneficial features, heme bears also toxic properties and an excess of heme is deleterious to cells due to its pro-oxidant features. For these reasons, cells and organisms have evolved several mechanisms to regulate heme concentration(4).

The control of heme homeostasis and oxidative stress appears particularly important in intestinal cells. The maintenance of the intestinal epithelial redox environment is essential for the activities of key physiological processes that include digestion and absorption, cell proliferation and apoptosis, and immune response. The fine tuning of the extracellular redox environment is also crucial in the intestinal stem cell niche that signals intestinal cell genesis(5). Accordingly, the disruption of intestinal redox homeostasis has been associated to the development of gut disorders(1,36), among which intestinal ulcers and cancer.

The control of intracellular heme levels in enterocytes was previously thought to occur through a balance among the uptake of heme from dietary sources, its biosynthesis,

utilization by hemoproteins, and catabolism by heme oxygenase (HO) (predominantly by the heme-inducible HO-1)(15). However, the expression of heme exporters, such as the Feline Leukemia Virus, subgroup C, Receptor 1 (FLVCR1) and the ATP-binding cassette, sub-family G, member 2 (ABCG2) in the intestine, suggests the existence of a mechanism of heme export from the enterocytes. The physiological significance of such secretory systems is unknown, but a likely hypothesis is that they may keep safe cells from the accumulation of an excess of heme, thus reducing cytotoxicity and representing a valuable system of cell protection.

Flvcr1a is one of the two isoforms codified by the Flvcr1 gene. FLVCR1a is a cell surface protein composed of 12 membrane-spanning domains. It is a member of the major-facilitator superfamily of secondary transporters, capable of transporting small solutes in response to chemiosmotic ion gradients(31). Flvcr1a mRNA is expressed ubiquitously with the highest expression observed in the liver, duodenum, kidney, lung, spleen, brain, placenta and bone marrow(15). The role of FLVCR1a as a heme exporter has been described in different cell types, including erythroid cells, macrophages and hepatocytes(2,14,25,33).

The present work demonstrates that FLVCR1a acts as a heme exporter in intestinal cells and that is crucial for the normal intestinal cell proliferation in vivo. Moreover, it demonstrates the importance of FLVCR1a for the maintenance of the peculiar homeostasis of proliferating intestinal cells, including the ability to counteract heme-mediated oxidative effects. Finally, it shows that Flvcr1a depletion is associated with a reduced animal survival in a mouse model of ulcerative colitis.

RESULTS

Generation of intestine specific conditional Flvcr1a-null mice.

In order to study the role of Flvcr1a in the intestine, an intestine specific conditional Flvcr1a-knockout mouse was generated. To this purpose, LoxP sites were introduced into the regions flanking Flvcr1 exon 1 to generate a floxed allele(33). Mice homozygous for the floxed allele are referred to as Flvcr1a$^{flox/flox}$. Flvcr1a$^{flox/flox}$ mice were then bred to transgenic Villin-Cre mice(7), expressing Cre ricombinase under the control of the Villin promoter. Following subsequent matings, Flvcr1a$^{flox/flox}$;Vil-Cre mice (referred to as Cre^{+} mice in the figures) were obtained. Flvcr1a$^{flox/flox}$ mice (referred to as Cre^{-} mice in the figures) were used as controls.

Polymerase chain reaction (PCR) assay on several adult Flvcr1a$^{flox/flox}$;Vil-Cre mouse tissues showed the presence of the wild-type Flvcr1a allele in all the organs analysed, except for the intestine (duodenum and colon-rectum are shown as representative intestinal regions) where the recombinant allele appeared, correspondent to the exon 1-excised Flvcr1a allele (Supplementary Figure S1A and Supplementary Table S1). However, both recombinant and non-recombinant alleles were detected in the intestine of the Flvcr1a$^{flox/flox}$;Vil-Cre mouse (Supplementary Figure S1A) indicating either that the recombination of the Flvcr1a$^{flox/flox}$ allele in intestinal mucosa cells is incomplete or that DNA from other cells not expressing the Cre ricombinase (muscle cells, endothelial cells, etc.) contributes to the signal of the intact Flvcr1a$^{flox/flox}$ allele.

Nevertheless, Flvcr1a transcript was strongly reduced in Flvcr1a$^{flox/flox}$;Vil-Cre intestine (duodenum and colon-rectum) respect to control animals (Supplementary Figure S1B).

Flvcr1a$^{flox/flox}$;Vil-Cre mice were viable and fertile, with normal sex ratio at birth. Haematoxylin-Eosin staining of duodenum, liver, spleen and kidney sections from two

month-old animals revealed no apparent morphological tissue abnormalities (Supplementary Figure S1C). Moreover, ten month-old mice colon-rectum sections appeared comparable to that of wild-type mice (Supplementary Figure S1D), excluding age-dependent defects in the morphology of Flvcr1a$^{flox/flox}$;Vil-Cre intestinal mucosa.

Two month-old mice were used for subsequent analyses.

FLVCR1a protein is located at the latero-apical side of intestinal cell membrane

The localization of heme and iron transporters in non-polarized and polarized cells and in the intestine has been carefully analysed(6,34). Nevertheless, very poor information is available about the precise cellular localization of FLVCR1a protein. Considering its role as the receptor for the feline leukaemia virus, a plasma membrane localization for this protein has been postulated and so far this hypothesis has been confirmed in FLVCR1a-overexpressing HEp-2 cells(35), in HepG2 cells(33) and in Hela cells(2).

In order to fill the gap in the knowledge of FLVCR1a localization on intestinal cells, human colon adenocarcinoma Caco2 cells stably expressing a C-terminal myc-tagged form of the murine FLVCR1a protein were analysed. The observation of non-polarized Caco2 cells confirmed the expected plasma membrane localization of FLVCR1a (Figure 1A and Supplementary Figure S2). Moreover, the analysis of polarized Caco2 cells revealed a latero-apical localization of the protein (Figure 1B).

Loss of Flvcr1a results in increased heme levels in intestinal cells.

As FLVCR1a is reported to act as a heme exporter in erythroid cells, macrophages and hepatocytes(2,14,25,33), a similar function for this protein was expected also in intestinal cells. To address this point, the expression of the heme-induced genes HO-1, ferroportin 1

(Fpn1) and H-ferritin (H-Ft) was assessed in Flvcr1a$^{flox/flox}$;Vil-Cre mice intestine as a read-out of heme content in intestinal cells. Duodenum was chosen as a representative intestinal region for the analysis. Increased HO-1 and Fpn1 mRNA levels were observed in the duodenum of Flvcr1a$^{flox/flox}$;Vil-Cre mice (Figure 2A). Moreover, H-Ft mRNA and protein levels were higher in Flvcr1a$^{flox/flox}$;Vil-Cre mice than in controls (Figure 2A, B).

To further confirm the role of FLVCR1a as a heme exporter in intestinal cells, cellular heme content was measured in Caco2 cells stably expressing a short hairpin RNA (shRNA) against Flvcr1a transcript (Supplementary Figure S3). Heme level was significantly higher in Flvcr1a depleted cells than in control cells expressing a scramble shRNA (Figure 2C).

Collectively, all the data support the idea that FLVCR1a acts as a heme exporter in intestinal cells as in other cell types. Moreover, they demonstrate that the lack of Flvcr1a in the intestine results in increased heme catabolism in intestinal cells.

Loss of Flvcr1a in the intestine does not affect dietary heme absorption.

Heme content in intestinal cells is accounted for by two main sources: dietary heme and heme derived from local biosynthesis. The role of FLVCR1a in the export of heme deriving from both these sources was analysed.

First, the effect of the lack of Flvcr1a on dietary heme absorption was assessed.

The intestinal absorption of a molecule is a multistep process involving its uptake from gut lumen, its retention in intestinal cell cytosol and its export towards the bloodstream.

To analyse the involvement of Flvcr1a in the export step of the heme absorption process, intestinal mucosa heme retention was measured in Flvcr1a$^{flox/flox}$;Vil-Cre mice following administration of an oral dose of ^{57}Fe labelled heme (^{57}Fe-heme). In case of defects in heme export, increased mucosal heme retention was expected. The analysis was focused on

duodenum as dietary heme absorption mainly occurs in this intestinal region(6) and ^{57}Fe, an iron isotope naturally occurring in animal tissues, was used as tracer due to its low natural abundance(9).

Ninety minutes after the administration of ^{57}Fe labelled heme, a higher amount of ^{57}Fe was detected in the duodenal mucosa of the administered mice as compared with vehicle-treated controls. The amount of heme-derived ^{57}Fe retained in the mucosa was comparable in Flvcr1a$^{flox/flox}$;Vil-Cre mice and Flvcr1a$^{flox/flox}$ controls (Figure 3A), suggesting that dietary heme export is poorly influenced by the presence or absence of FLVCR1a in the duodenum. To further address this point, Flvcr1a$^{flox/flox}$;Vil-Cre mice were maintained on an heme-supplemented diet for one week and the mRNA levels of the transcriptionally heme-regulated gene Fpn1 was measured. As expected, Fpn1 mRNA levels increased following heme-supplementation (Figure 3B). Nevertheless, the increase was comparable in Flvcr1a$^{flox/flox}$;Vil-Cre mice and in controls, indicating that dietary heme retention, and consequently heme export, was similar in the two genotypes.

The lack of FLVCR1a involvement in the export of heme deriving from diet was supported also by other indications. Analyses on tissues iron levels, mainly determined by dietary heme and iron absorption, did not reveal any abnormalities in Flvcr1a$^{flox/flox}$;Vil-Cre mice (Figure 3C and Supplementary Figure S4). Moreover, Flvcr1a$^{flox/flox}$;Vil-Cre mice showed normal haematological parameters (Figure 3D). Finally, the mRNA level of the liver hormone Hepcidin, the master regulator of iron absorption, was comparable in Flvcr1a$^{flox/flox}$;Vil-Cre mice and controls (Figure 3E).

Collectively, all the data indicate that the lack of Flvcr1a in the duodenum does not affect dietary heme absorption.

In agreement with this conclusion, an enhanced duodenal HO-1 mRNA level and HO activity, as well as Fpn1 mRNA level was observed in wild-type mice maintained on a heme-

supplemented diet for one week, while Flvcr1a mRNA level was unaffected, confirming that, following uptake, dietary heme was mainly catabolised inside the enterocytes rather than exported (Supplementary Figure S5).

FLVCR1a mediates the export of de novo synthesized heme.

As mentioned before, in addition to dietary heme absorption, local heme biosynthesis represents a second process contributing to heme supply in enterocytes. Thus, the involvement of FLVCR1a in the export of de novo synthesized heme was examined.

In order to address this point, wild-type mice were orally administered with the heme-biosynthesis inducer aminolevulinic acid (ALA) for three days and the expression of HO-1 and Flvcr1a was measured as an indication of heme catabolism and export, respectively. An increase of both HO-1 and Flvcr1a mRNA levels was observed, indicating that the excess of heme produced upon stimulation of heme biosynthesis in the intestine is partly degraded and partly exported (Figure 4A). To confirm this hypothesis, in vitro experiments on Caco2 cells were performed. ALA treatment for two days was able to induce both HO-1 and Flvcr1a mRNA levels in these cells (Figure 4B).

Moreover, five hours following ALA treatment the heme content of Caco2 cells expressing a shRNA against Flvcr1a was significantly higher than in ALA-treated control cells expressing a scramble shRNA (Figure 4C).

Together, the data show an involvement of FLVCR1a in the export of the novo synthesized heme.

Loss of Flvcr1a impairs normal cell proliferation in vivo

Besides important beneficial features, heme bears toxic properties(22,32) and an excessive release of heme by hemoproteins and mitochondria is associated with deleterious effects on cellular functions and oxidative status.

To get an insight into the biological importance of FLVCR1a-mediated heme export, heme effects on intestinal oxidative status and cell proliferation were examined in Flvcr1a$^{flox/flox}$;Vil-Cre mice.

Despite higher intestinal mRNA levels of the antioxidant enzyme superoxide dismutase 1 (Sod1) in Flvcr1a$^{flox/flox}$;Vil-Cre mice than in controls (Figure 5A and Supplementary Figure S6), the intestinal SOD1 protein levels were comparable in the two genotypes (Figure 5B). Moreover, the intestinal mRNA levels of thioredoxin reductase (Txnrd1) and gamma glutamyl cysteine synthetase (γ-GCS) were comparable in Flvcr1a$^{flox/flox}$;Vil-Cre and Flvcr1a$^{flox/flox}$ mice (Figure 5A and Supplementary Figure S6).

To directly assess the level of reactive oxygen species in the intestine, tissue homogenates and fresh intestinal rings were analysed. The results obtained did not reveal differences between Flvcr1a$^{flox/flox}$;Vil-Cre mice and controls (Figure 5C and Supplementary Figure S6). Similarly, intestinal lipid peroxidation was comparable in the two genotypes (Supplementary Figure S6). Thus, the lack of Flvcr1a is not associated to increased oxidative stress in the intestine of mice under steady state conditions.

More interesting results were obtained analysing cell proliferation in mice intestinal sections. Indeed, a lower amount of Ki67-positive cells was observed in the intestinal mucosa of the Flvcr1a$^{flox/flox}$;Vil-Cre mice as compared to the Flvcr1a$^{flox/flox}$ mucosa (Figure 5D), indicating that the loss of Flvcr1a impairs intestinal cell proliferation in vivo.

Loss of Flvcr1a impairs the peculiar homeostasis of proliferating tumor cells

To further address the role of Flvcr1a in intestinal cell proliferation and homeostasis, the effect of Flvcr1a loss in proliferating adenocarcinoma Caco2 cells was dissected.

The measure of apoptosis and the analysis of cell cycle phases did not reveal any apparent alteration in Caco2 cells stably expressing a shRNA against Flvcr1a transcript as compared to control cells expressing a scramble shRNA (Supplementary Figure S7), indicating that in a context of abnormal proliferation the lack of Flvcr1a is not sufficient to further perturb the already altered rate of cell division. Nevertheless, several parameters were impaired in Flvcr1a-depleted Caco2 cells.

First, the measure of the redox status indicated increased oxidative stress in Flvcr1a-depleted Caco2 cells than in control cells (Figure 6A). Interestingly, despite the higher amount of reactive oxygen species and an increase in SOD1 mRNA level (Figure 6B), SOD1 protein levels in Flvcr1a-depleted cells were comparable to that observed in control cells (Figure 6C). This indicates that proliferating cells lacking Flvcr1a are unable to efficaciously counteract the increase of excessive reactive oxygen species derived from heme accumulation.

Second, a perturbation of cell-cell contacts was observed in Flvcr1a-depleted cells, as demonstrated by the decrease of cell monolayer permeability (Figure 6D) and the concomitant increase of the tight junction claudin V protein expression (Figure 6E).

Finally, the metabolic activity of Caco2 cells stably expressing a shRNA against Flvcr1a transcript was lower than that observed in control cells expressing a scramble shRNA (Figure 6F).

The data reported herein collectively demonstrate that the export of heme mediated by FLVCR1a is crucial to maintain the proliferation of normal intestinal cells in vivo. Moreover, in proliferating tumor cells FLVCR1a allows the maintenance of crucial features for their

peculiar homeostasis, such as the ability to counteract heme-mediated oxidative effects, to regulate cell-cell contacts and to preserve high metabolic activity.

Flvcr1a depletion impairs mice survival to ulcerative colitis.

Several studies pointed to a correlation between imbalance in the cellular oxidative status and inflammation, bowel diseases and cancer(26). Ulcerative colitis (UC) is an idiopathic disease characterized by mucosal inflammation of the large bowel. The etiopathogenesis remains uncertain, but oxidative stress and oxidative cellular damage play key roles. An intermittent disease evolution characterized by a flare-up/remission cycle can be observed in UC patients, with increased mucosa cellular turnover occurring during the remission periods(29). To investigate whether the enhanced oxidative stress in proliferating cells and the decreased intestinal mucosa cells proliferation associated to Flvcr1a loss could influence the response to this pathology, Flvcr1a$^{flox/flox}$;Vil-Cre mice and controls were challenged with dextran sulphate sodium (DSS), a chemical known to induce colitis in rodents that is clinically and histologically reminiscent of human UC(19,29). Both groups of mice developed the disease, showing similar short-term survival, colon-cecum length shortening, weight loss, inflammatory infiltrates and disease scoring during the seven days of DSS treatment (Figure 7A-D). Thus, the “flare-up phase” of the disease seemed to be unaffected by the loss of Flvcr1a. Nevertheless, analysing the animals ten days after the end of the DSS treatment, a period correspondent to the remission phase, the survival of Flvcr1a$^{flox/flox}$;Vil-Cre mice appeared significantly compromised as compared with that of Flvcr1a$^{flox/flox}$ controls (Figure 7E). Indeed, the majority of Flvcr1a$^{flox/flox}$;Vil-Cre animals died and only a limited number of these mice overcome this phase, showing colon-rectum length, body weight and disease score

comparable to that of Flvcr1a$^{flox/flox}$ mice (Supplementary Table S2 and Supplementary Figure S8).

Collectively, the data reported herein indicate that the intestinal mucosa cell defects associated to the loss of Flvcr1a reduce the long term survival of Flvcr1a$^{flox/flox}$;Vil-Cre animals to ulcerative colitis, likely because of an impaired ability of these mice to regenerate the mucosal integrity in the sites of damage.

DISCUSSION

FLVCR1a is a heme exporter ubiquitously expressed in the organism. Previous studies have described the importance of FLVCR1a function particularly in erythroid cells, lymphocytes(23) and hepatocytes(2,14,25,33). The present work establishes for the first time a role for FLVCR1a in the export of heme excess from intestinal cells to limit heme deleterious effects. Particularly, FLVCR1a collaborates to the maintenance of heme homeostasis in both normal intestinal cells and in intestine-derived tumor cells. The data reported describe a previously unknown involvement of Flvcr1a in the maintenance of the normal intestinal cell proliferation rate. Furthermore, they show that FLVCR1a is important to maintain the peculiar state of intestine-derived tumor cells, including high metabolic activity and ability to counteract oxidative stress. Finally, the results obtained show a decreased survival of intestinal conditional Flvcr1a-null mice to ulcerative colitis, a bowel disease affecting a wide portion of human population(36).

The first point described in this study is the role of Flvcr1a as a heme exporter in the intestine.

The destiny of dietary heme taken up from gut lumen has been a matter of debate for years. Data reported in this work demonstrate that FLVCR1a does not export heme deriving from dietary sources. Accordingly, the presence or absence of Flvcr1a does not affect dietary heme absorption. The observed apical localization of FLVCR1a protein in polarized Caco2 cells further discourages the possibility that FLVCR1a could participate to the export of dietary heme in the bloodstream. These results do not exclude the possibility that other transporters could export dietary heme from intestinal cells. However, the induction of HO-1 upon dietary heme supplementation strongly supports the idea that most of dietary heme undergoes

degradation after the entry in the enterocytes. Conversely, our data show the involvement of FLVCR1a in the export of heme excess released by mitochondria during heme biosynthesis. This is in agreement with previously reported data on the role of Flvcr1a in hepatocytes(33). Thus, Flvcr1a has a specific role in heme handling associated to endogenous heme biosynthesis and its function cannot be compensated by increased heme catabolism. Further studies are required to elucidate whether FLVCR1a-mediated heme export is directed towards gut lumen in order to detoxify intestinal cells from excessive heme accumulation or, alternatively, whether an exchange of heme among neighbouring cells could take place to distribute this molecule along the intestinal mucosa.

A second point emerging from the analysis of Caco2 cells lacking FLVCR1a is that this protein contributes to maintain the high metabolic activity(11) and the low cell-cell adhesion(18) typical of proliferating tumor cells. Several studies showed that proliferating cancer cells reduce their mitochondrial activity to favour a glycolisis based-metabolism(11). However, other studies exist, demonstrating that mitochondrial activity, including respiratory chain activity and heme biosynthesis, still retain a great importance in proliferating tumor cells(13). It could be hypothesised that a balance between heme export from mitochondria to cytosol, mediated by the FLVCR1b isoform, and that out of the cell, executed by FLVCR1a protein, must be maintained to preserve mitochondrial functions and, consequently, the enhanced metabolic activity of proliferating cells. In agreement with this hypothesis, a similar function for Flvcr1a has been described in the erythropoietic system(20).

Regarding cell-cell contacts, the latero-apical localization of FLVCR1a could suggest yet unknown direct or indirect interactions of this transmembrane protein with members of the tight-junction complexes and/or adhesion molecules.

Whatever the mechanism could be, the general effect of Flvcr1a depletion is a reduction of some of the typical features of proliferating cells. This is further supported by the observation in vivo of a decreased proliferation of the intestinal mucosa cells.

The analysis of Caco2 cells lacking Flvcr1a reveals another important function for this heme exporter in proliferating cells that is its contribution to limit cell oxidative stress.

Proliferating tumour cells show adaptation to high levels of reactive oxygen species(17). However, an excessive accumulation of these species could be deleterious for their wellness(17).

Several studies indicate that the excess of heme favours the establishment of cellular oxidative stress(22). In addition, oxidative stress conditions are often associated with heme release from hemoproteins, this event further contributing to exacerbate the cytotoxic context(12). For these reasons, most if not all forms of oxidative stress are associated with a rapid increase in the rate of cellular heme catabolism through the induction of HO-1 expression. By coupling oxidative stress to HO-1 activation, cells would limit heme-driven cytotoxicity(12). In this context, heme export through FLVCR1a represents a complementary strategy exploited by cells to counteract heme-associated toxic effects. These findings are in agreement with previously published data about the role of FLVCR1a in the liver(33) and the regulation of Flvcr1a during hypoxia(10), a condition related to redox disturbances.

In vivo, the involvement of FLVCR1a in the protection of intestinal mucosa from oxidative stress does not emerge. Several explanations could be proposed. First, as FLVCR1a carries out this function together with HO and many other antioxidant proteins, it is possible that in a physiological context the sole absence of Flvcr1a expression is not sufficient to perturb the complex and sophisticated system designated to maintain intestinal redox status. Second, it cannot be excluded that FLVCR1a role becomes crucial in proliferating cells, a limited

population in the intestinal mucosa, mainly restricted to crypts. In this case, the whole analysis of the tissue could hide differences in a limited group of cells in the mucosa.

A very interesting point emerging from the analysis of intestinal conditional Flvcr1a-null mice is a decreased number of proliferating cells in their intestinal mucosa. The loss of obvious abnormalities in the intestinal mucosa of these animals suggests that, under physiologic condition, the alteration of cellular renewal due to Flvcr1a deficiency is well compensated. Nevertheless, the appearance of gut abnormalities with increasing age cannot be excluded. On the other hand, our data demonstrate that this role of Flvcr1a has a crucial impact in pathologic situations, as the response of mice to ulcerative colitis.

The use of DSS to induce ulcerative colitis in mice has been widely documented(29) and the model is considered clinically and histologically reminiscent of human UC(19,29). The possibility that the DSS effects observed in intestinal conditional Flvcr1a-null mice are due to an enhanced permeability of their mucosa to this toxic compound is unlikely. Indeed, although permeability assays have been performed in vitro, the fact that monolayers of Caco2 cells lacking Flvcr1a show a lower permeability than that of control cells suggests that the mucosa of intestinal conditional Flvcr1a-null mice could be more resistant, rather than permeable, to DSS entry. Moreover, the dose of DSS employed caused so dramatic damages that an eventual difference in tissue permeability would have negligible consequences.

DSS effects are known to be largely due to inflammatory events elicited by this compound. Intestinal conditional Flvcr1a-null mice show an immunological response comparable to that of controls. This was expected as Flvcr1a depletion is restricted to the intestinal mucosa of these mice.

The considerations reported herein are collectively supported by the observation of a similar susceptibility to DSS during the “damage phase” between intestinal conditional Flvcr1a-null

mice and control animals. The different survival observed between the two genotypes could be ascribed to a defect in the ability to recover the damage in mice lacking Flvcr1a, a process mainly involving proliferation rather than tissue permeability to DSS or inflammation. Thus, the possible mechanism proposed to explain the higher survival of mice expressing Flvcr1a observed in this work is that the presence of FLVCR1a can preserve intestinal mucosa cell proliferation and the wellness of proliferating cells, allowing regeneration of the mucosa at the site of damage.

The present work shows that, by exerting the export of endogenously synthesised heme, FLVCR1a guarantees the normal intestinal cell proliferation and contribute to the maintenance of the mucosal integrity. The activity of Flvcr1a appears particularly important in the context of ulcerative colitis, where this heme exporter becomes crucial for animal survival, likely thanks to its ability to sustain mucosal regeneration after the injury.

Beyond the role of Flvcr1a in mice survival to ulcerative colitis, these findings open the intriguing possibility that Flvcr1a could exert protection against various forms of gut pathologies. On the other hand, the effects of the block of Flvcr1a functions in tumor proliferating cells could prepare the ground for future studies on Flvcr1a in cancer.

INNOVATION

The present work represents the first description of Flvcr1a function in the intestine and an advance in the understanding of heme metabolism in this tissue. The reported data indicate that Flvcr1a-mediated heme export does not contribute to dietary heme absorption processes and unravel a new role for heme export in the control of intestinal mucosa renewal and in the maintenance of proliferating tumor cells homeostasis, including redox status. Furthermore, the data reported enlighten the importance of Flvcr1a function in mice survival to ulcerative colitis, opening the intriguing possibility that Flvcr1a could exert protection against various forms of gut pathologies.

MATERIALS AND METHODS

Animals

Intestine specific conditional Flvcr1a-knockout mice were generated in the mixed 129Sv x C57BL/6 genetic background. Transgenic Villin-Cre mice in the C57BL/6 genetic background were from Charles River Laboratories International, Inc. (Wilmington MA, USA).

Wild-type mice in the Sv129 background were used for some experiments.

Mice fed on a heme-supplemented diet received drinking water supplemented with 250 μmol/L Hemin (Sigma-Aldrich, Milano, Italy) and 2 mmol/L L-Arginin (Sigma-Aldrich, Milano, Italy).

Mice treated with ALA were given drinking water supplemented with 2 mg/mL of δ-aminolevulinic acid (ALA; A3785; Sigma-Aldrich, Milano, Italy), as described previously(24).

All experiments were approved by the animal studies committee of the University of Torino (Italy).

Haematological parameters

Blood was collected from anesthetized mice by cardiac puncture and haematological parameters were determined according to standard procedures on an automatic analyzer.

Haematoxylin and Eosin staining and Immunohistochemistry

Standard procedures were followed for haematoxylin and eosin (H&E) staining of kidney, liver, spleen and duodenum 5 μm thick paraffin sections,

For colon-rectum, the tissue (from the cecum till the anal sphincter) was removed, washed with 0.1 M phosphate buffer saline (PBS) and opened longitudinally to expose the mucosa. Following over-night fixation in 4% formaldehyde at 4ºC, colon-rectum specimens were arranged in a "Swiss" roll, processed and embedded in paraffin. 5 µm thick tissue sections were stained with H&E. Alternatively, colon-rectum slides were immunostained, according to standard procedures, with a rabbit antibody to Ki-67 (dilution 1:250, Abcam, Cambridge, UK) after antigen retrieval with 10 mM citric acid pH 6 for 5 minutes at 95ºC.

Tissue iron measurement

Total Fe was determined using inductively coupled plasma mass spectrometry (ICP-MS) as described previously(8).

Tissue iron was also measured by the 4,7-diphenyl-1, 10-phenantroline disulphonic acid (BPS)-based colorimetric method and by Perls' stain, as previously reported(21).

^{57}Fe-heme absorption

^{57}Fe-heme absorption analyses were performed as described previously (8,9).

Heme oxygenase activity

HO activity was evaluated in tissue microsomal fractions by measuring bilirubin production as previously described(8).

Western blotting

Western blotting analysis of H-ferritin and SOD1 protein in mouse intestine and of SOD1 and Claudin V in Caco2 cells was performed on total duodenum or cells lysates, respectively,

according to standard procedures using an antibody against H-ferritin(27), or SOD1 (Santa Cruz Biotechnology Inc., Dallas, Texas, USA) or Claudin V (Abcam, Cambridge, UK) .

RNA extraction and real-time PCR analysis

RNA extraction and quantitative real time PCR (qRT-PCR) were performed as previously reported(8) using the Universal Probe Library system (Roche, Milano, Italy). Primers and probes were designed using the ProbeFinder software (www.roche-applied-science.com).

For Flvcr1a specific primers and the probe were designed using Primer Express Sofware Version 3.0 (Applied Biosystems).

Transcript abundance, normalized to 18S mRNA expression (for mouse tissues) or to beta-actin mRNA expression (for Caco2 cells), is expressed as a fold increase over a calibrator sample.

Cell culture

The Caco2 cells (ATCC: HTB-37™) were propagated in appropriate standard conditions.

To induce polarization $1*10^5$ cells/cm^2 were seeded on transwell permeable supports (Corning, NY) endowed with a polyester membrane of 0.33cm^2 and pores of 0.4µm. Full polarization was considered to be achieved about 20 days post-confluence.

To activate heme biosynthesis, Caco2 cells were treated for 5 or 48 hours with 5mM δ-aminolevulinic acid (ALA; A3785; Sigma-Aldrich, Milano, Italy).

Flvcr1a silencing

For gene silencing, a shRNA (TRC Lentiviral pLKO.1 Human Flvcr1 shRNA set RHS4533-NM_014053, clone TRCN0000059599, Thermo Fisher Scientific, Inc. Waltham MA, USA) targeting the first exon of human Flvcr1 gene was used to specifically down-regulate

Flvcr1a. For control cells, a pLKO.1 scramble shRNA (Thermo Fisher Scientific, Inc. Waltham MA, USA) was used.

Following lentiviral transduction, cells were selected with 0.02µg/ml puromycin.

Flvcr1a-Myc expression

To obtain myc-tagged FLVCR1a expressing cells, Caco2 cells were transduced with a lentiviral pCCL.ET vector carrying the mouse Flvcr1a cDNA fused to the Myc epitope under the enhanced transthyretin promoter.

Immunofluorescence

Immunofluorescence was performed according to standard procedures with a home made mouse antibody to Myc. A goat anti-mouse Alexa Fluor 488 conjugated secondary antibody (Molecular Probes, Inc., Eugene, OR) was employed. Cell nuclei were stained with 4',6-diamidin-2-fenilindolo (DAPI, Sigma-Aldrich, Milano, Italy) while cell membrane with Alexa Fluor 594 conjugated wheat germ agglutinin (WGA, Thermo Fisher Scientific, Inc. Waltham MA, USA). For analyses on polarized cells, the polyester filter of transwell inserts was removed and mounted with ProLong antifade reagent (Molecular Probes, Inc., Eugene, OR). Cells were examined with a Zeiss Observer-Z1 microscope, equipped with the ApoTome system (Zeiss, Jena, Germany). Images and Z-stacks were acquired and processed with the digital image processing software Axiovision (Zeiss, Jena, Germany).

Measurement of heme concentration

Intracellular heme concentration was measured using a fluorescence assay, as previously reported(30). Briefly, Caco2 cells untreated or treated for 5 hours with ALA were collected and 2M oxalic acid was added to them. Samples were heated at 100°C for 30 minutes leading

to iron removal from heme. Fluorescence (wavelength: excitation 400nm - emission 662nm) of the resultant protoporphyrin was assessed on a Glomax Multi Detection System (Promega Corporation, Madison WI, USA).

The endogenous protoporphyrin content (measured in parallel unheated samples in oxalic acid) was subtracted. Data were normalized to total protein concentration in each sample. Results were expressed as pmol of heme/mg total protein.

Measurement of intracellular reactive oxygen species accumulation

Accumulation of reactive oxygen species (ROS) in Caco2 cells and in mouse intestine was assessed using the oxidant-sensitive fluorescent dye 29,79-dichlorodihydrofluoroscein diacetate (H_2DCFDA; Molecular Probes, Inc., Eugene, OR). Caco2 cells were incubated with 5μM H_2DCFDA in cell medium for 30 min at 37 °C under 5% CO_2 atmosphere. Then, cells were washed twice with 0.1 M PBS and lysed in 0.1M PBS. A quantity of lysate correspondent to 10μg protein was analysed. Mouse intestine was dissected after transcardial perfusion of mice with PBS. Mouse intestinal homogenates were prepared in PBS containing butylated hydroxytoluene. After centrifugation at 6000 rpm for 10 minutes at 4°C, a quantity of lysates correspondent to 300μg protein was incubated with 20μM H_2DCFDA in PBS for 30 min at 37 °C under 5% CO_2 atmosphere.

Fluorescence was recorded at excitation and emission wavelengths of 485 and 530 respectively on a Glomax Multi Detection System (Promega Corporation, Madison WI, USA). Background fluorescence of cells or homogenates, respectively, untreated with H_2DCFDA was subtracted from the total fluorescence. Results were expressed as arbitrary fluorescence unit.

MTT assay

$8*10^3$ Caco2 cells were plated on 96 multi-wells, and every 24 h cell growth was evaluated by 3-(4,5-Dimethylthiazol-2-yl)-2,5-Diphenyltetrazolium Bromide (MTT) assay (Roche, Milano, Italy) according to the manufacturer's instructions.

Cell cycle and apoptosis analysis.

For cell cycle analysis $8x10^5$ cells were harvested by centrifugation at 1200 rpm for 5 minutes at 4°C and fixed with cold 70% ethanol O.N. at -20°C. Samples were pelleted, treated with 0.1 mg RNAse (type I-A) (Sigma-Aldrich, Milano, Italy) and resuspended in PBS containing propidium iodide (Sigma-Aldrich, Milano, Italy). For apoptosis analysis 5 $x10^5$ cells were collected, washed in PBS, resuspended in 10 mM Hepes, 150 mM NaCl, 5 mM $CaCl_2$ buffer, and labelled with annexinV (BD Biosciences) for 20 minutes. Then, 2 µl propidium iodide (1 mg/ml) (Sigma-Aldrich, Milano, Italy) was added.

AnnexinV emission was detected in the green channel (525nm) and propidium iodide in the red channel (575nm) on a FACSCalibur (BD Biosciences, Milano, Italy) using CellQuest Software (BD Biosciences, Milano, Italy).

TEER measure.

The permeability of the cell monolayer was monitored by measuring the trans-epithelial electrical resistance (TEER) using an epithelial voltohmeter (World Precision Instrument, Sarasota, Florida, USA). At the indicated time point, the medium TEER of three independent measures for every sample was recorded. Data are expressed as $Ohm*cm^2$.

Induction of colitis

Induction of colitis was achieved as described previously(28). Briefly, the animals were divided into groups and mice receiving DSS were administered 3 % w/v DSS (dextran sulphate sodium salt, MW 36000-50000, MP Biomedicals LLC, Illkirch Cedex, France)

dissolved in autoclaved tap water for 7 days. Healthy control animals received autoclaved tap water. At day 7, tap water was administered to all mice. A part of mice per group was sacrified at day 8. The remaining animals were administered tap water for nine additional days and sacrified at day 17. Colon-rectum sections were stained with H&E. Damage scores on colon-rectum slides were assigned in a blinded fashion, on an scale of 0 to 6, as reported previously(19), where 0 = no signs of damage; 1 = few inflammatory cells, no signs of epithelial degeneration; 2 = mild inflammation, few signs of epithelial degeneration; 3 = moderate inflammation, few epithelial ulcerations; 4 = moderate to severe inflammation, ulcerations in more than 25% of the tissue section; 5 = moderate to severe inflammation, large ulcerations of more than 50% of the tissue section; 6 = severe inflammation and ulcerations of more than 75% of the tissue section.

Statistical Analysis

Results were expressed as mean ±SEM. Statistical analyses were performed using one-way or two-way analysis of variance followed by the Bonferroni correction for multiple group comparisons. An unpaired Student's *t*-test was used when only two groups were compared. A *P* value of less than 0.05 was regarded as significant.

ACKNOWLEDGEMENTS

The authors would like to thank Sonia Levi for purchasing the anti H-Ferritin antibody, Simonetta Geninatti Crich and Silvio Aime for heme absorption experiments, Valentina Pala and Annalisa Camporeale for help with some experiments.

This work was supported by the Telethon grant GGP12082 and by the AIRC grant IG14599 to ET.

AUTHOR DISCLOSURE STATEMENT

The authors declare that no competing financial interests exist.

AUTHOR CONTRIBUTIONS

VF design and perform the experiments, made the analyses and wrote the paper; MF analysed histological preparations; LS and FA were involved in study design; ET designed the experiments, analysed the data and wrote the paper.

LIST OF ABBREVIATIONS

ABCG2 (ATP-binding cassette, sub-family G, member 2)

ALA (aminolevulinic acid)

BPS (4,7-diphenyl-1, 10-phenantroline disulphonic acid)

DAPI (4',6-diamidin-2-fenilindolo)

DSS (dextran sulphate sodium)

FLVCR1a (Feline Leukemia Virus, subgroup C, Receptor 1a)

Fpn1 (ferroportin 1)

γ-GCS (gamma glutamyl cysteine synthetase)

H&E (haematoxylin and eosin)

H-Ft (H-ferritin)

^{57}Fe-heme (^{57}Fe labelled heme)

HO (heme oxygenase)

ICP-MS (coupled plasma mass spectrometry)

MDA (malondialdehyde)

MTT (3-(4,5-Dimethylthiazol-2-yl)-2,5-Diphenyltetrazolium Bromide)

PBS (phosphate buffer saline)

PCR (Polymerase chain reaction)

PFA (paraformaldehyde)

shRNA (short hairpin RNA)

SOD1 (superoxide dismutase 1)

TEER (trans-epithelial electrical resistance)

Txnrd1 (thioredoxin reductase)

UC (ulcerative colitis)

WGA (wheat germ agglutinin)

REFERENCES

1. Aw TY. Intestinal glutathione: determinant of mucosal peroxide transport, metabolism, and oxidative susceptibility. *Toxicol Appl Pharmacol* 204: 320-8, 2005.
2. Chiabrando D, Marro S, Mercurio S, Giorgi C, Petrillo S, Vinchi F, Fiorito V, Fagoonee S, Camporeale A, Turco E, Merlo GR, Silengo L, Altruda F, Pinton P, Tolosano E. The mitochondrial heme exporter FLVCR1b mediates erythroid differentiation. *J Clin Invest* 122: 4569-79, 2012.
3. Chiabrando D, Mercurio S, Tolosano E. Heme and erythropoieis: more than a structural role. *Haematologica* 99: 973-83, 2014.
4. Chiabrando D, Vinchi F, Fiorito V, Mercurio S, Tolosano E. Heme in pathophysiology: a matter of scavenging, metabolism and trafficking across cell membranes. *Front Pharmacol* 5: 61, 2014.
5. Circu ML, Aw TY. Redox biology of the intestine. *Free Radic Res* 45: 1245-66, 2011.
6. Dunn LL, Suryo Rahmanto Y, Richardson DR. Iron uptake and metabolism in the new millennium. *Trends Cell Biol* 17: 93-100, 2007.
7. el Marjou F, Janssen KP, Chang BH, Li M, Hindie V, Chan L, Louvard D, Chambon P, Metzger D, Robine S. Tissue-specific and inducible Cre-mediated recombination in the gut epithelium. *Genesis* 39: 186-93, 2004.
8. Fiorito V, Geninatti Crich S, Silengo L, Aime S, Altruda F, Tolosano E. Lack of Plasma Protein Hemopexin Results in Increased Duodenal Iron Uptake. *PLoS One* 8: e68146, 2013.
9. Fiorito V, Geninatti Crich S, Silengo L, Altruda F, Aime S, Tolosano E. Assessment of iron absorption in mice by ICP-MS measurements of (57)Fe levels. *Eur J Nutr* 51: 783-9, 2012.
10. Fiorito V, Neri F, Pala V, Silengo L, Oliviero S, Altruda F, Tolosano E. Hypoxia controls Flvcr1 gene expression in Caco2 cells through HIF2alpha and ETS1. *Biochim Biophys Acta* 1839: 259-64, 2014.
11. Formentini L, Martinez-Reyes I, Cuezva JM. The mitochondrial bioenergetic capacity of carcinomas. *IUBMB Life* 62: 554-60, 2010.
12. Gozzelino R, Jeney V, Soares MP. Mechanisms of cell protection by heme oxygenase-1. *Annu Rev Pharmacol Toxicol* 50: 323-54, 2010.
13. Hooda J, Cadinu D, Alam MM, Shah A, Cao TM, Sullivan LA, Brekken R, Zhang L. Enhanced heme function and mitochondrial respiration promote the progression of lung cancer cells. *PLoS One* 8: e63402, 2013.
14. Keel SB, Doty RT, Yang Z, Quigley JG, Chen J, Knoblaugh S, Kingsley PD, De Domenico I, Vaughn MB, Kaplan J, Palis J, Abkowitz JL. A heme export protein is required for red blood cell differentiation and iron homeostasis. *Science* 319: 825-8, 2008.
15. Khan AA, Quigley JG. Control of intracellular heme levels: heme transporters and heme oxygenases. *Biochim Biophys Acta* 1813: 668-82, 2011.
16. Krishnamurthy P, Xie T, Schuetz JD. The role of transporters in cellular heme and porphyrin homeostasis. *Pharmacol Ther* 114: 345-58, 2007.
17. Liou GY, Storz P. Reactive oxygen species in cancer. *Free Radic Res* 44: 479-96, 2010.
18. Martin TA, Jiang WG. Loss of tight junction barrier function and its role in cancer metastasis. *Biochim Biophys Acta* 1788: 872-91, 2009.

19. Melgar S, Karlsson L, Rehnstrom E, Karlsson A, Utkovic H, Jansson L, Michaelsson E. Validation of murine dextran sulfate sodium-induced colitis using four therapeutic agents for human inflammatory bowel disease. *Int Immunopharmacol* 8: 836-44, 2008.
20. Mercurio S, Petrillo S, Chiabrando D, Bassi ZI, Gays D, Camporeale A, Vacaru A, Miniscalco B, Valperga G, Silengo L, Altruda F, Baron MH, Santoro MM, Tolosano E. Heme exporter Flvcr1 regulates expansion and differentiation of committed erythroid progenitors by controlling intracellular heme accumulation. *Haematologica*, 2015.
21. Morello N, Tonoli E, Logrand F, Fiorito V, Fagoonee S, Turco E, Silengo L, Vercelli A, Altruda F, Tolosano E. Haemopexin affects iron distribution and ferritin expression in mouse brain. *J Cell Mol Med* 13: 4192-204, 2009.
22. Morimatsu H, Takahashi T, Shimizu H, Matsumi J, Kosaka J, Morita K. Heme Proteins, Heme Oxygenase-1 and Oxidative Stress. In: *Oxidative Stress - Molecular Mechanisms and Biological Effects*. edited by Lushchak V. InTech; 2012. pp. 109-124.
23. Philip M, Funkhouser SA, Chiu EY, Phelps SR, Delrow JJ, Cox J, Fink PJ, Abkowitz JL. Heme exporter FLVCR is required for T cell development and peripheral survival. *J Immunol* 194: 1677-85, 2015.
24. Phillips JD, Jackson LK, Bunting M, Franklin MR, Thomas KR, Levy JE, Andrews NC, Kushner JP. A mouse model of familial porphyria cutanea tarda. *Proc Natl Acad Sci U S A* 98: 259-64, 2001.
25. Quigley JG, Yang Z, Worthington MT, Phillips JD, Sabo KM, Sabath DE, Berg CL, Sassa S, Wood BL, Abkowitz JL. Identification of a human heme exporter that is essential for erythropoiesis. *Cell* 118: 757-66, 2004.
26. Reuter S, Gupta SC, Chaturvedi MM, Aggarwal BB. Oxidative stress, inflammation, and cancer: how are they linked? *Free Radic Biol Med* 49: 1603-16, 2010.
27. Santambrogio P, Cozzi A, Levi S, Rovida E, Magni F, Albertini A, Arosio P. Functional and immunological analysis of recombinant mouse H- and L-ferritins from Escherichia coli. *Protein Expr Purif* 19: 212-8, 2000.
28. Seril DN, Liao J, Ho KL, Warsi A, Yang CS, Yang GY. Dietary iron supplementation enhances DSS-induced colitis and associated colorectal carcinoma development in mice. *Dig Dis Sci* 47: 1266-78, 2002.
29. Seril DN, Liao J, Yang GY, Yang CS. Oxidative stress and ulcerative colitis-associated carcinogenesis: studies in humans and animal models. *Carcinogenesis* 24: 353-62, 2003.
30. Sinclair PR, Gorman N, Jacobs JM. Measurement of heme concentration. *Curr Protoc Toxicol* Chapter 8: Unit 8.3, 2001.
31. Tailor CS, Willett BJ, Kabat D. A putative cell surface receptor for anemia-inducing feline leukemia virus subgroup C is a member of a transporter superfamily. *J Virol* 73: 6500-5, 1999.
32. Tolosano E, Fagoonee S, Morello N, Vinchi F, Fiorito V. Heme scavenging and the other facets of hemopexin. *Antioxid Redox Signal* 12: 305-20, 2010.
33. Vinchi F, Ingoglia G, Chiabrando D, Mercurio S, Turco E, Silengo L, Altruda F, Tolosano E. Heme exporter FLVCR1a regulates heme synthesis and degradation and controls activity of cytochromes P450. *Gastroenterology* 146: 1325-38, 2014.
34. Yanatori I, Tabuchi M, Kawai Y, Yasui Y, Akagi R, Kishi F. Heme and non-heme iron transporters in non-polarized and polarized cells. *BMC Cell Biol* 11: 39, 2010.

35. Yanatori I, Yasui Y, Miura K, Kishi F. Mutations of FLVCR1 in posterior column ataxia and retinitis pigmentosa result in the loss of heme export activity. *Blood Cells Mol Dis* 49: 60-6, 2012.
36. Zhu H, Li YR. Oxidative stress and redox signaling mechanisms of inflammatory bowel disease: updated experimental and clinical evidence. *Exp Biol Med (Maywood)* 237: 474-80, 2012.

FIGURE LEGENDS

Figure 1. FLVCR1a protein is located at the latero-apical side of intestinal cells membrane. (A) Undifferentiated FLVCR1a-myc expressing Caco2 cells stained with DAPI (i) and an antibody to myc (ii). The merged image is shown on iii. Bar= 20µm. (B) Polarized FLVCR1a-myc expressing Caco2 cells stained with DAPI (i) and an antibody to myc (ii). The merged image is shown on iii. The lateral view (XZ image) (iv) is made up by the addition of 50 consecutive z-stack images in the y-axis. Nuclei are in blue and FLVCR1a-myc protein is in green. In this image, the cell apical side is up, whereas the cell basal side is down. Latero-apical localization of FLVCR1a-myc protein can be appreciated. Bar= 40µm.

Figure 2. Lack of Flvcr1a results in increased heme levels in intestinal cells. (A) qRT-PCR analysis of HO-1, Fpn1 and H-Ft expression in the duodenum of Flvcr1a$^{flox/flox}$ (Cre-) and Flvcr1a$^{flox/flox}$;Vil-Cre (Cre+) mice. Transcript abundance, normalized to 18S RNA expression, is expressed as a fold increase over a calibrator sample. Data represent mean ± SEM, n= 5; *=P<0.05. (B) Representative Western blot of H-Ft expression in the duodenum of Flvcr1a$^{flox/flox}$ (Cre-) and Flvcr1a$^{flox/flox}$;Vil-Cre (Cre+) mice. Band intensities were measured by densitometry and normalized to actin expression. Densitometry data represent mean ± SEM, n=3; *=P<0.05. (C) Heme content in Caco2 cells in which the expression of Flvcr1a was down-regulated using a specific shRNA. Values are expressed as pmol heme/ mg protein. Data represent mean ± SEM, n=10; *=P<0.05.

Figure 3. Lack of Flvcr1a in the intestine does not affect dietary heme absorption. (A) ^{57}Fe retention in the duodenal mucosa of Flvcr1a$^{flox/flox}$ (Cre-) and Flvcr1a$^{flox/flox}$;Vil-Cre (Cre+) mice measured by ICP-MS 90 minutes after oral administration of a solution containing 20 mmol/L ^{57}Fe labelled heme (^{57}Fe-heme). Control mice were administered

vehicle solution and represented the "0" time point of the experiment. Values are expressed as μg ^{57}Fe/ g tissue. Data represent mean ± SEM, n=3 for each experimental point; *=P<0.05, **=P<0.01 (comparing control mice with the corresponding group of ^{57}Fe-heme-administered mice). (B) qRT-PCR analysis of Fpn1 expression in the duodenum of Flvcr1a$^{flox/flox}$ (Cre-) and Flvcr1a$^{flox/flox}$;Vil-Cre (Cre+) mice maintained on a standard diet or on a heme-supplemented diet for one week. Transcript abundance, normalized to 18S RNA expression, is expressed as a fold increase over a calibrator sample. Data represent mean ± SEM, n=3; *=P<0.05. (C) Total iron content in the spleen, muscle, liver, kidney and duodenum of Flvcr1a$^{flox/flox}$ (Cre-) and Flvcr1a$^{flox/flox}$;Vil-Cre (Cre+) mice measured by ICP-MS (for the spleen, muscle, liver, kidney) or by the BPS-based colorimetric method (for the duodenum). Values obtained by ICP-MS are expressed as μg iron/g wet tissue while values obtained by the BPS-based colorimetric method as μg iron/g dry tissue. Data represent mean ± SEM, n=5. (D) Reticulocytes percentage (%Ret), haematocrit (HCT), mean corpuscular volume (MCV), platelet count (PLT), red blood cell count (RBC) and white blood cell count (WBC) in blood sample from Flvcr1a$^{flox/flox}$ (Cre-) and Flvcr1a$^{flox/flox}$;Vil-Cre (Cre+) mice. Units of measure for each parameter are reported in the table. Data represent mean ± SEM, n=3. (E) qRT-PCR analysis of Hepc expression in the liver of Flvcr1a$^{flox/flox}$ (Cre-) and Flvcr1a$^{flox/flox}$;Vil-Cre (Cre+) mice. Transcript abundance, normalized to 18S RNA expression, is expressed as a fold increase over a calibrator sample. Data represent mean ± SEM, n=6.

Figure 4. FLVCR1a mediates the export of de novo synthesized heme. (A) qRT-PCR analysis of HO-1 and Flvcr1a expression in the duodenum of wild-type mice maintained on a δ-aminolevulinic acid (ALA)-supplemented diet for 3 days. Control mice were maintained on a standard diet and represented the "0" time point of the experiment. Transcript abundance,

normalized to 18S RNA expression, is expressed as a fold increase over a calibrator sample. Data represent mean ± SEM, n=3; **=P<0.01, ***=P<0.001. (B) qRT-PCR analysis of HO-1 and Flvcr1a expression in Caco2 cells untreated (-) or treated (+) with δ-aminolevulinic acid (ALA) for 48 hours. Data represent mean ± SEM, n=5; *=P<0.05. (C) Heme content in Caco2 cells in which the expression of Flvcr1a was down-regulated using a specific shRNA. Heme biosynthesis was stimulated with δ-aminolevulinic acid (ALA) for 5 hours. Caco2 cells untreated (-) or treated (+) with δ-aminolevulinic acid (ALA) are compared. Values are expressed as pmol heme/ mg protein. Data represent mean ± SEM, n=6; **=P<0.01, ***=P<0.001.

Figure 5. Loss of Flvcr1a impairs normal cell proliferation in vivo. (A) qRT-PCR analysis of SOD1, γ-GCS and Txnrd1 expression in the colon-rectum of Flvcr1a$^{flox/flox}$ (Cre-) and Flvcr1a$^{flox/flox}$;Vil-Cre (Cre+) mice. Transcript abundance, normalized to 18S RNA expression, is expressed as a fold increase over a calibrator sample. Data represent mean ± SEM, n=5; *=P<0.05. (B) Representative Western blot of SOD1 expression in the intestine of Flvcr1a$^{flox/flox}$ (Cre-) and Flvcr1a$^{flox/flox}$;Vil-Cre (Cre+) mice. Band intensities were measured by densitometry and normalized to vinculin expression. Densitometry data represent mean ± SEM, n=3. (C) ROS amount measured by detection of H_2DCFDA fluorescence in intestinal homogenates from Flvcr1a$^{flox/flox}$ (Cre-) and Flvcr1a$^{flox/flox}$;Vil-Cre (Cre+) mice. Values are expressed as arbitrary fluorescence unit. Data represent mean ± SEM, n=6. (D) Representative sections of the colon-rectum of a Flvcr1a$^{flox/flox}$ (Cre-) (i, iii, v) and a Flvcr1a$^{flox/flox}$;Vil-Cre (Cre+) mouse (ii, iv, vi) stained with an antibody to Ki-67. Enlarged details of sections iii, iv are shown in v, vi respectively. The Ki-67-positive signal was more intense in the Flvcr1a$^{flox/flox}$ (Cre-) mouse than in the Flvcr1a$^{flox/flox}$;Vil-Cre (Cre+) animal. Bar i, ii = 200μm; bar iii, iv = 100 μm. The number of Ki-67-positive cells per crypt on the

total number of cells per crypt is shown as a percentage in the graph. Data represent mean ± SEM, n=3; *=P<0.05.

Figure 6. Lack of Flvcr1a impairs the peculiar homeostasis of proliferating tumor cells. (A) Intracellular ROS accumulation measured by detection of H_2DCFDA fluorescence in Caco2 cells in which the expression of Flvcr1a was down-regulated using a specific shRNA. Values are expressed as arbitrary fluorescence unit. Data represent mean ± SEM, n=5; **=P<0.01. (B) qRT-PCR analysis of SOD1 expression in Caco2 cells in which the expression of Flvcr1a was down-regulated using a specific shRNA. Transcript abundance, normalized to βActin RNA expression, is expressed as a fold increase over a calibrator sample. Data represent mean ± SEM, n=6; *=P<0.05. (C) Western blot of SOD1 expression in undifferentiated and polarized Caco2 cells in which the expression of Flvcr1a was down-regulated using a specific shRNA. Actin expression is shown as a loading control. Data are representative of three independent experiments. (D) Representative TEER measure on Caco2 cells in which the expression of Flvcr1a was down-regulated using a specific shRNA. Data are expressed as Ohm*cm^2. At the indicated time point, the medium TEER of three independent measures for every sample was recorded. Data represent mean ± SEM, n=12; ***=P<0.001. Data are representative of three independent experiments. (E) Western blot of Claudin V expression in undifferentiated and polarized Caco2 cells in which the expression of Flvcr1a was down-regulated using a specific shRNA. Actin expression is shown as a loading control. Data are representative of three independent experiments. (F) MTT-based proliferation analysis of Caco2 cells in which the expression of Flvcr1a was down-regulated using a specific shRNA. Values are expressed as MTT absorbance. Data represent mean ± SEM, n=3 for each experimental point; *=P<0.05, ***=P<0.001 (comparing cells at different

time points with the corresponding cell group at "day 0"), $^{##}$=P<0.01, $^{###}$=P<0.001 (comparing scramble-shRNA expressing cells with Flvcr1a-shRNA expressing cells).

Figure 7. Flvcr1a depletion impairs mice survival to ulcerative colitis. (A) Colon length of Flvcr1a$^{flox/flox}$ (Cre-) and Flvcr1a$^{flox/flox}$;Vil-Cre (Cre+) mice at day 8 of the experiment (one day after the cessation of DSS administration). Vehicle-treated mice represented the "0" time point of the experiment. Data represent mean ± SEM, n=5; **=P<0.01, ***=P<0.001. (B) Body weight of Flvcr1a$^{flox/flox}$ (Cre-) and Flvcr1a$^{flox/flox}$;Vil-Cre (Cre+) mice administered with DSS and analysed at day 0 and day 8 of the experiment. Data represent mean ± SEM, n=12; **=P<0.01, ***=P<0.001. (C) Representative sections of the colon-rectum of Flvcr1a$^{flox/flox}$ (Cre-) (i) and Flvcr1a$^{flox/flox}$;Vil-Cre (Cre+) (ii) mice treated with DSS and stained with H&E. Colon-rectum was dissected at day 8 of the experiment (one day after the cessation of DSS administration). Similar inflammatory infiltrates can be observed in the two genotypes. Bar= 100μm. (D) Representative sections of the colon-rectum of two Flvcr1a$^{flox/flox}$ (Cre-) (i, v) and two Flvcr1a$^{flox/flox}$;Vil-Cre (Cre+) mice (ii, vi) treated (v, vi) or not (i, ii) with DSS and stained with H&E. Colon-rectum was dissected at day 8 of the experiment (one day after the cessation of DSS administration). Higher magnification of sections i, v, ii, vi are shown in iii, iv, vii, viii respectively. Bar i, ii, v, vi = 1000μm; bar iii, iv, vii, viii = 200 μm. The disease score, shown in the graph, was assigned analysing colon-rectum sections of Flvcr1a$^{flox/flox}$ (Cre-) and Flvcr1a$^{flox/flox}$;Vil-Cre (Cre+) mice at day 8 of the experiment (one day after the cessation of DSS administration). Vehicle-treated mice represented the "0" time point of the experiment. Data represent mean ± SEM, n=5; ***=P<0.001. (E) Percentage survival of Flvcr1a$^{flox/flox}$ (Cre-) and Flvcr1a$^{flox/flox}$;Vil-Cre (Cre+) mice treated with DSS for 7 days followed by one or ten additional days with water. Data are presented as a Kaplan-Meier plot, n=12; *=P<0.05.

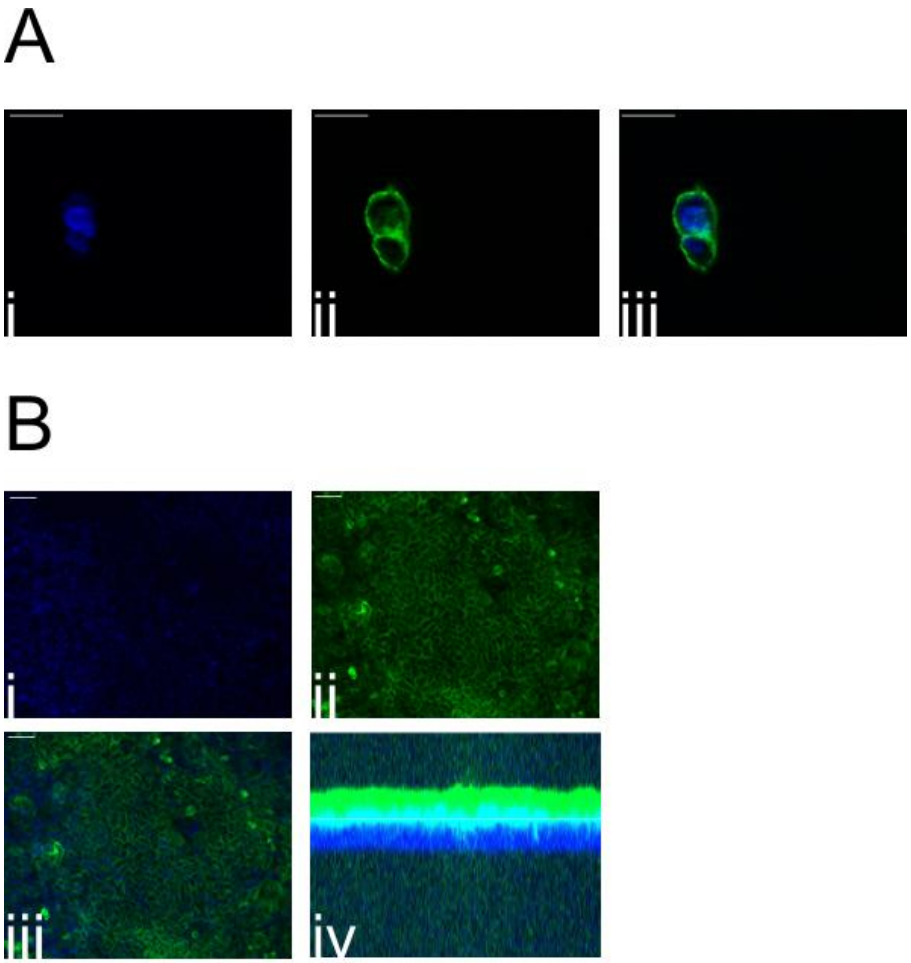

Figure 1

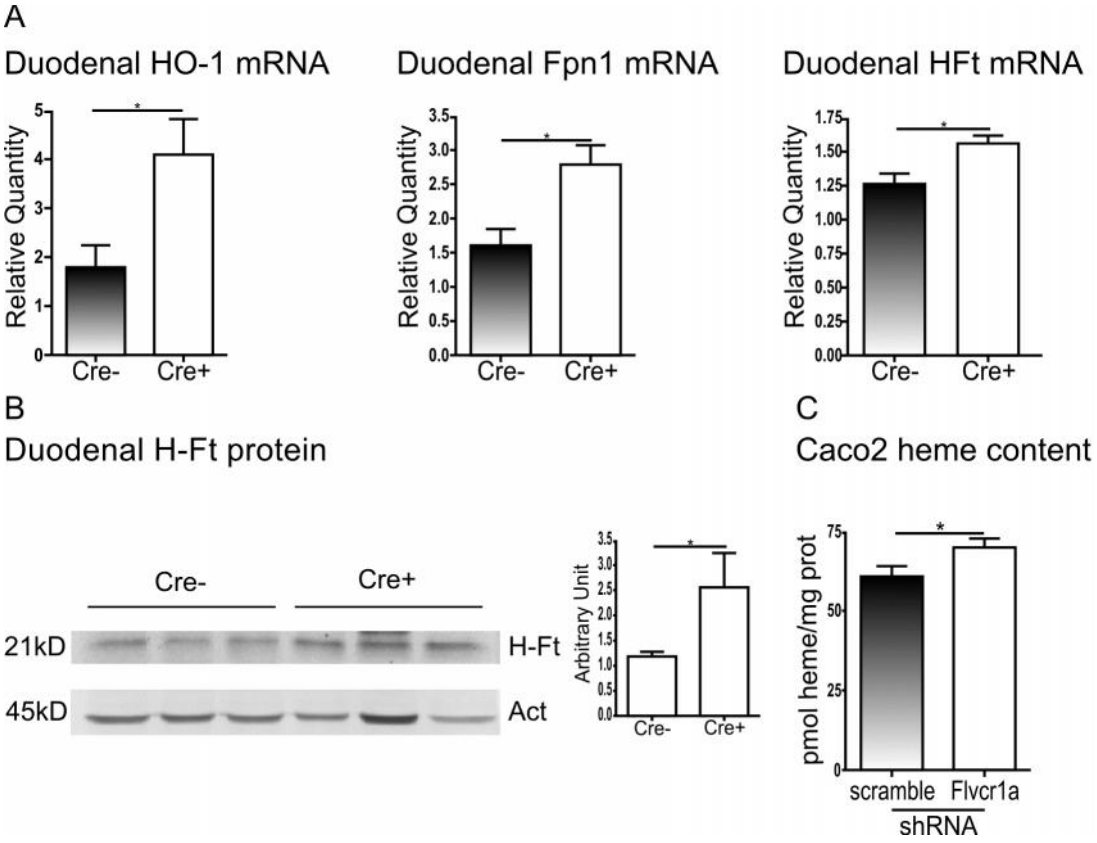
A
Duodenal HO-1 mRNA
Relative Quantity
Cre-
Cre+
Duodenal Fpn1 mRNA
Relative Quantity
Cre-
Cre+
Duodenal HFt mRNA
Relative Quantity
Cre-
Cre+
B
Duodenal H-Ft protein
Cre-
Cre+
21kD
H-Ft
45kD
Act
Arbitrary Unit
Cre-
Cre+
C
Caco2 heme content
pmol heme/mg prot
scramble
Flvcr1a
shRNA

Figure 2

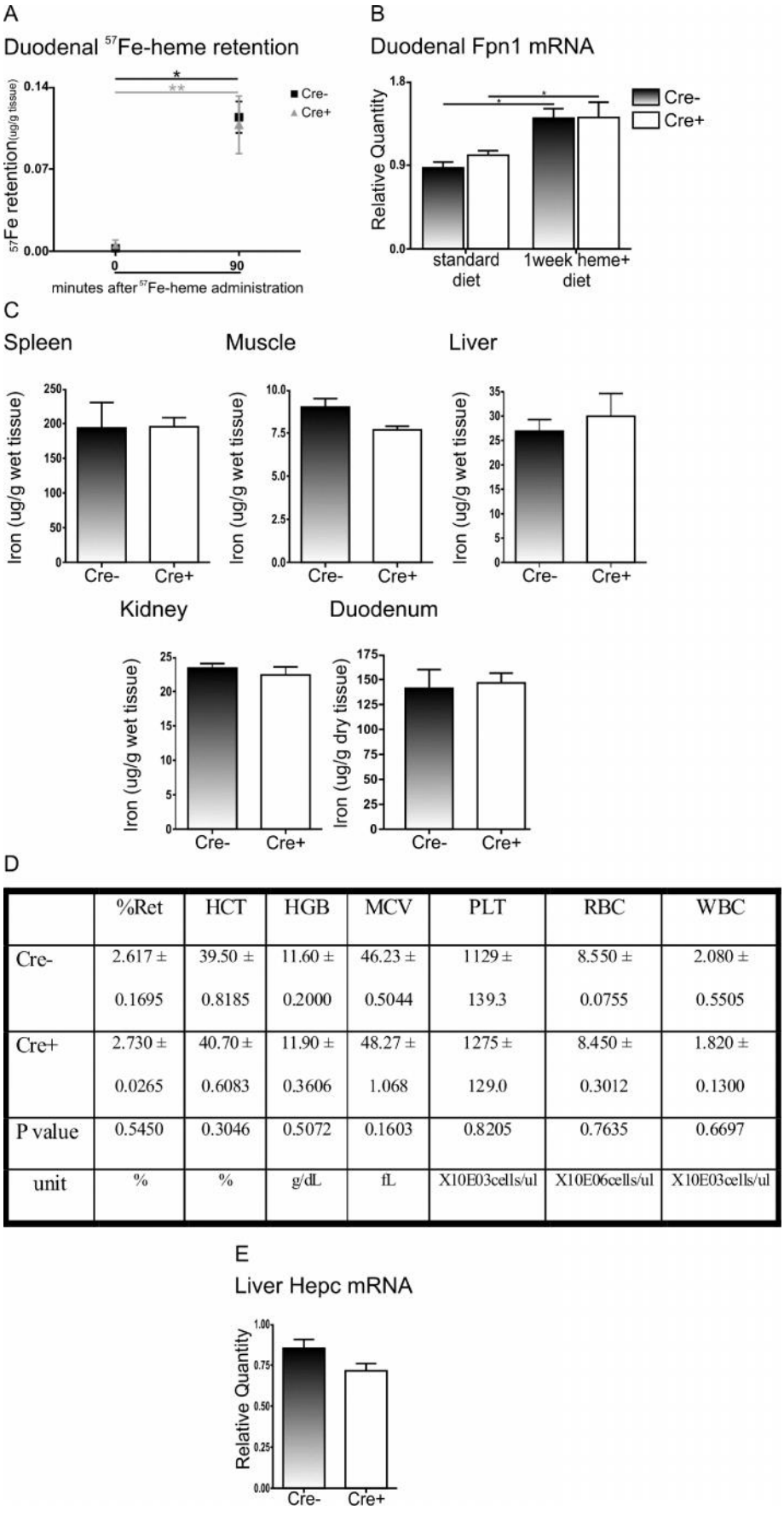

	%Ret	HCT	HGB	MCV	PLT	RBC	WBC
Cre-	2.617 ± 0.1695	39.50 ± 0.8185	11.60 ± 0.2000	46.23 ± 0.5044	1129 ± 139.3	8.550 ± 0.0755	2.080 ± 0.5505
Cre+	2.730 ± 0.0265	40.70 ± 0.6083	11.90 ± 0.3606	48.27 ± 1.068	1275 ± 129.0	8.450 ± 0.3012	1.820 ± 0.1300
P value	0.5450	0.3046	0.5072	0.1603	0.8205	0.7635	0.6697
unit	%	%	g/dL	fL	X10E03cells/ul	X10E06cells/ul	X10E03cells/ul

Figure 3

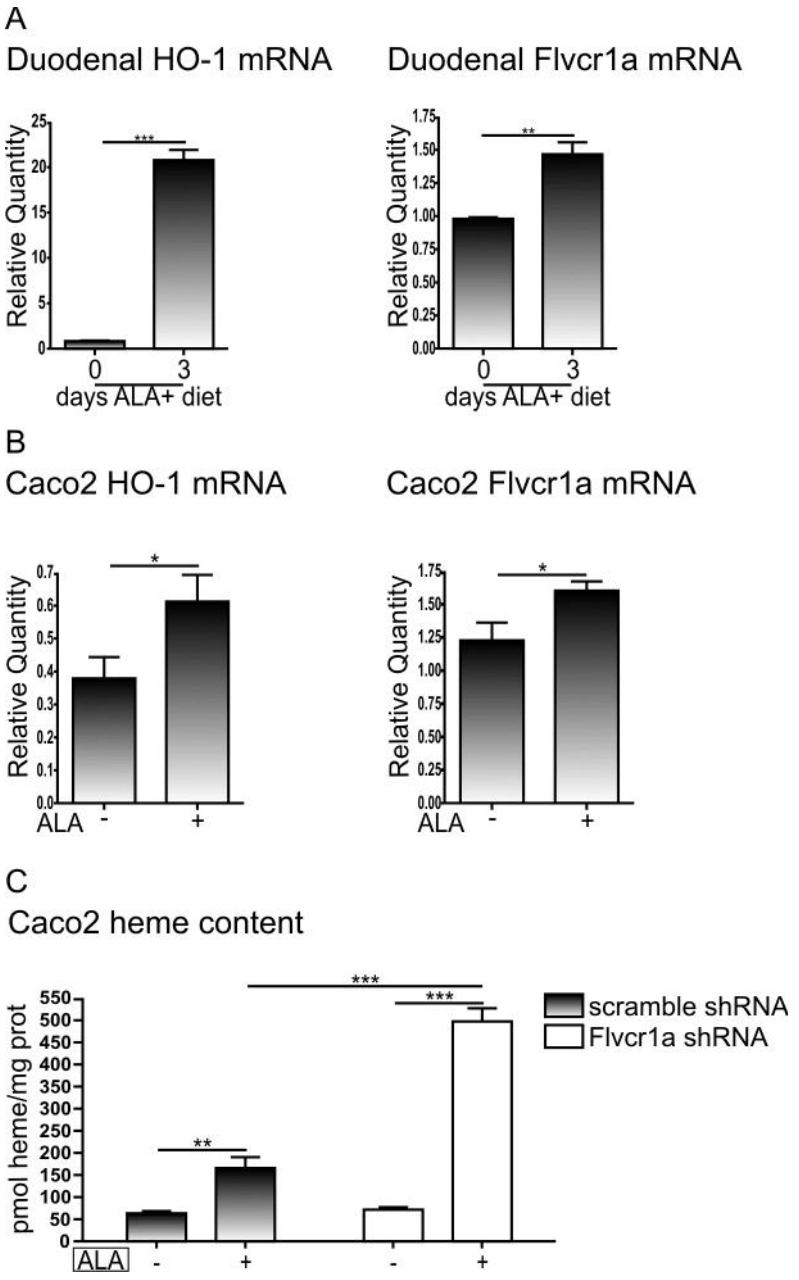
A
Duodenal HO-1 mRNA
Duodenal Flvcr1a mRNA
Relative Quantity
***
**
0
3
days ALA+ diet
B
Caco2 HO-1 mRNA
Caco2 Flvcr1a mRNA
*
ALA
-
+
C
Caco2 heme content
pmol heme/mg prot
scramble shRNA
Flvcr1a shRNA

Figure 4

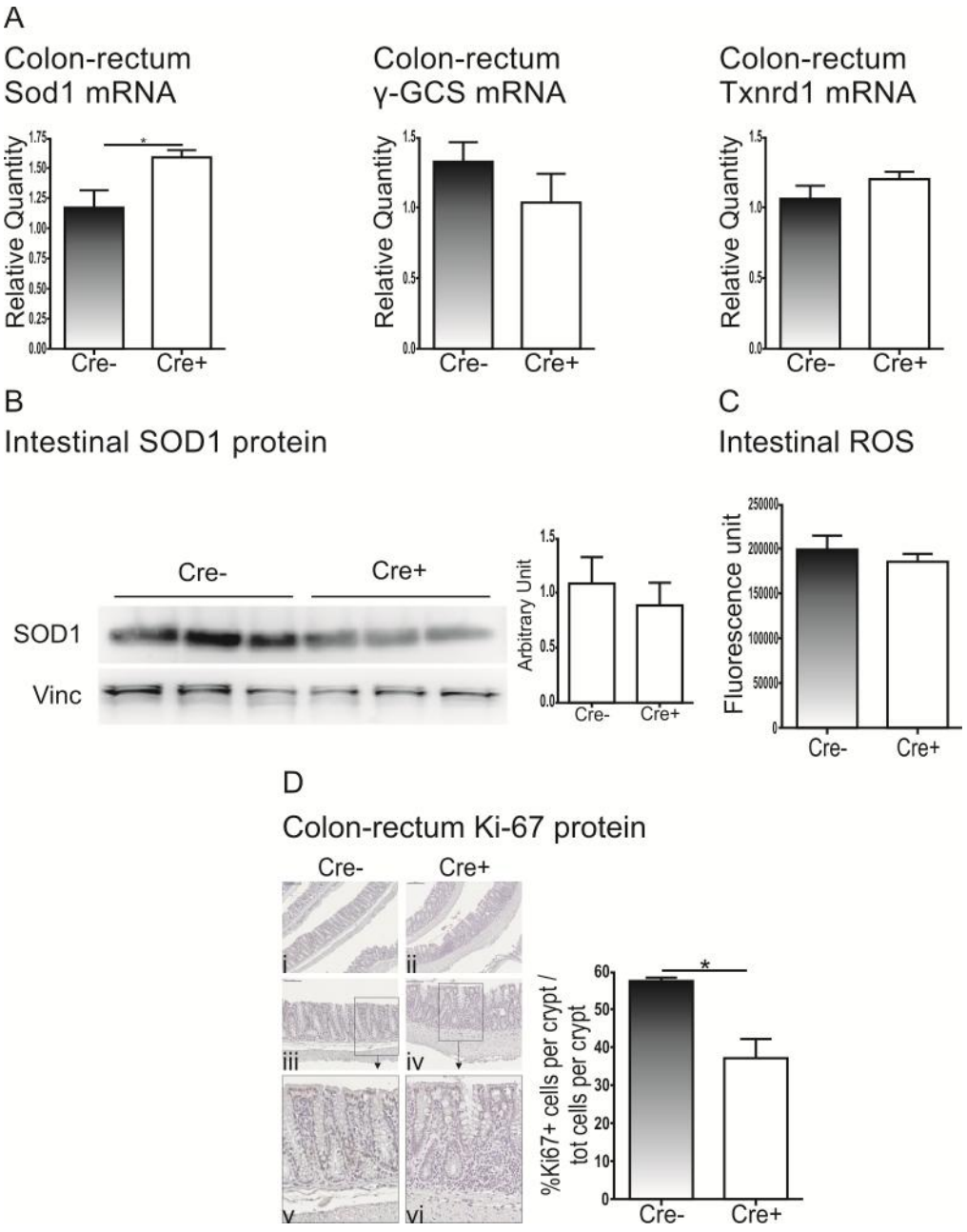
A
Colon-rectum
Sod1 mRNA
Relative Quantity
Cre-
Cre+
Colon-rectum
γ-GCS mRNA
Relative Quantity
Cre-
Cre+
Colon-rectum
Txnrd1 mRNA
Relative Quantity
Cre-
Cre+
B
Intestinal SOD1 protein
Cre-
Cre+
SOD1
Vinc
Arbitrary Unit
Cre-
Cre+
C
Intestinal ROS
Fluorescence unit
Cre-
Cre+
D
Colon-rectum Ki-67 protein
Cre-
Cre+
i
ii
iii
iv
v
vi
%Ki67+ cells per crypt /
tot cells per crypt
Cre-
Cre+

Figure 5

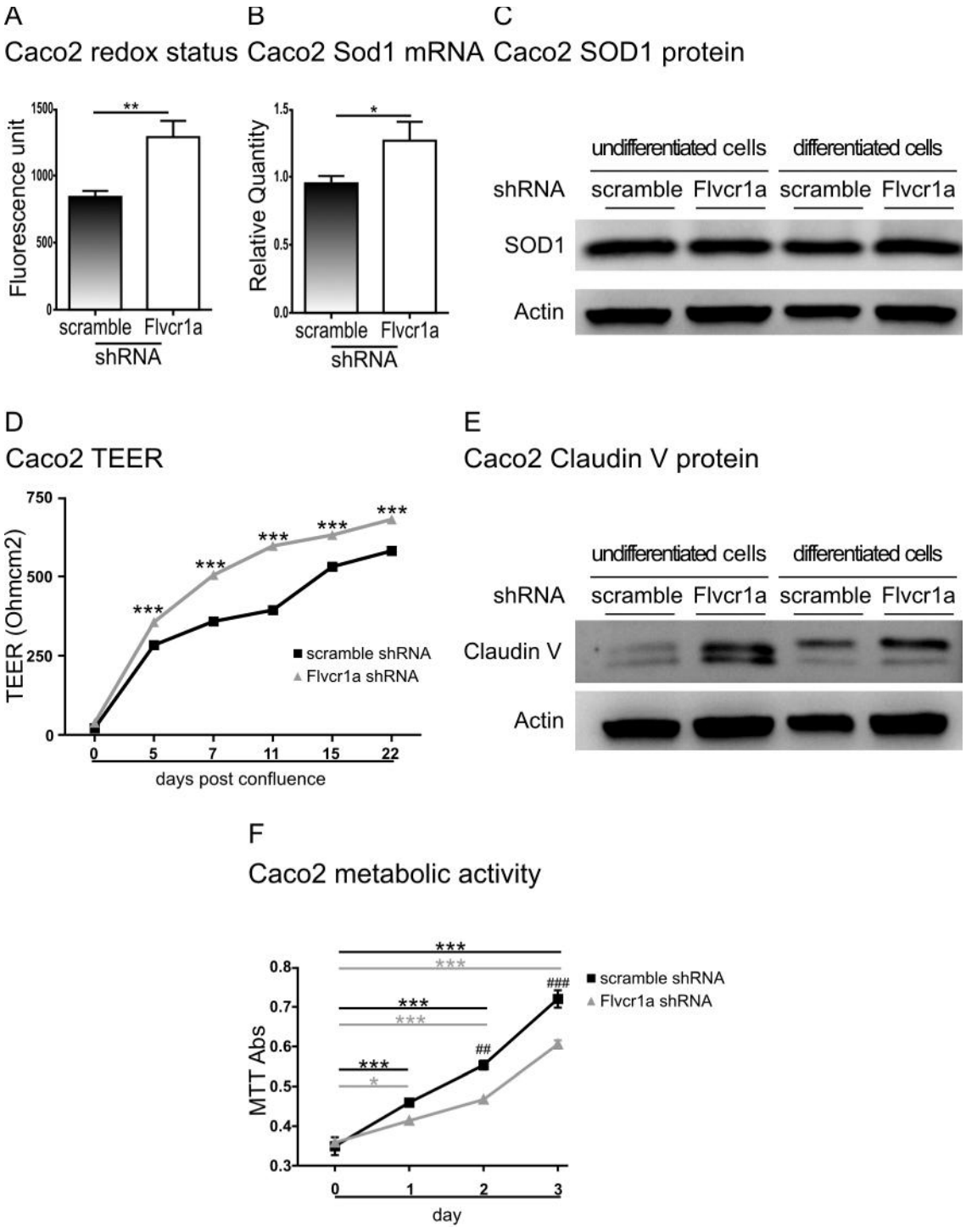
A
Caco2 redox status
Fluorescence unit
1500
1000
500
0
**
scramble
Flvcr1a
shRNA
B
Caco2 Sod1 mRNA
Relative Quantity
1.5
1.0
0.5
0.0
*
scramble
Flvcr1a
shRNA
C
Caco2 SOD1 protein
undifferentiated cells
differentiated cells
shRNA
scramble
Flvcr1a
scramble
Flvcr1a
SOD1
Actin
D
Caco2 TEER
TEER (Ohmcm2)
750
500
250
0
***
scramble shRNA
Flvcr1a shRNA
0
5
7
11
15
22
days post confluence
E
Caco2 Claudin V protein
undifferentiated cells
differentiated cells
shRNA
scramble
Flvcr1a
scramble
Flvcr1a
Claudin V
Actin
F
Caco2 metabolic activity
MTT Abs
0.8
0.7
0.6
0.5
0.4
0.3
***
***
###
##
*
scramble shRNA
Flvcr1a shRNA
0
1
2
3
day

Figure 6

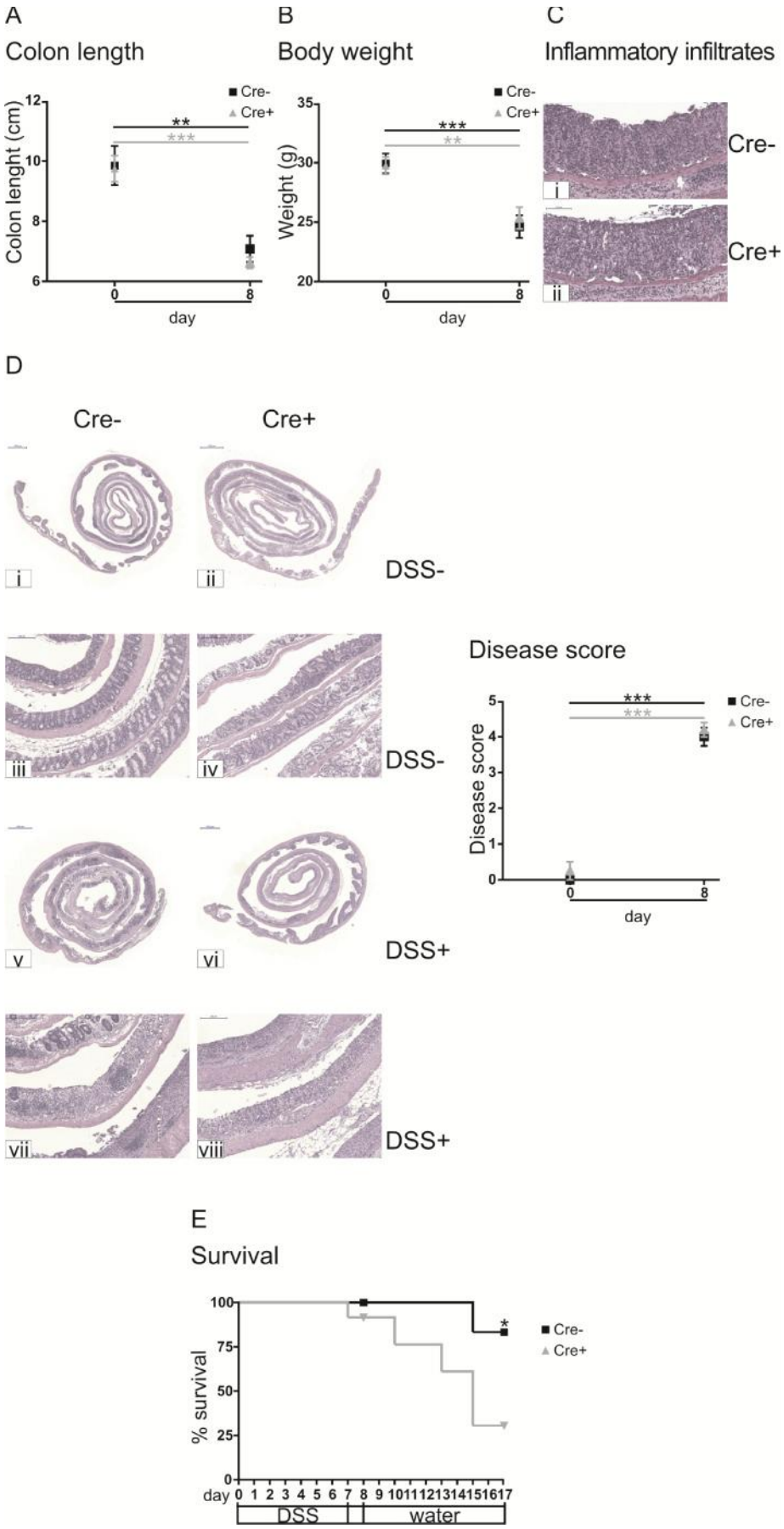
A
Colon length
Colon lenght (cm)
Cre-
Cre+
day
B
Body weight
Weight (g)
C
Inflammatory infiltrates
Cre-
Cre+
D
Cre-
Cre+
DSS-
DSS-
DSS+
DSS+
Disease score
Disease score
E
Survival
% survival
day
DSS
water

Figure 7